

The Formation of Whiskers on Electroplated Tin Containing Copper

K.-W. Moon, M. E. Williams, C. E. Johnson, G. R. Stafford,
C.A. Handwerker, and W. J. Boettinger

Metallurgy Division, MSEL, NIST, Gaithersburg, MD 20899-8555, USA

The probability of whisker growth on as-grown tin(Sn) electrodeposits has been measured as a function of copper(Cu) addition to a commercial bright methanesulfonate electrolyte. To provide reproducible plating conditions and to approximate flow conditions in commercial strip plating, a rotating disk electrode assembly was used. A fixed plating current at 25 °C was used to produce deposits 3 μm and 10 μm thick. Two substrates were used: free standing 250 μm thick pyrophosphate Cu deposits and 40 nm thick fine grain Cu evaporation deposited on silicon(Si) (100) wafer. Electrolyte Cu²⁺ concentrations from 0 to 25 x 10⁻³ mol/L produced deposits with average Cu compositions between 0 % and 3.3 % mass fraction, respectively. In the absence of Cu additions, no whiskers were observed on either substrate after 60 days of room temperature aging. With Cu additions, no whiskers were observed on the Cu-coated Si substrates, but whiskers were observed within two days on the pyrophosphate Cu substrates increasing to a density of 10²/mm² for the highest Cu contents. The deposits on the pyrophosphate Cu and Cu evaporated Si(100) substrates had different preferred orientations: (103) and (101) respectively, but the effect of Cu on the deposit microstructure was the same. The increase in Cu content reduced the Sn grain size from 0.65 μm to 0.2 μm in the deposits independent of substrate. Much of the Cu in the deposits occurred as Cu-rich particles on the Sn grain boundaries. The primary correlation observed was that Sn-Cu deposits with (103) preferred orientation were most likely to form whiskers.

Keywords: Sn whisker, electroplated Sn, Pb-free solder

1. Introduction

Tin(Sn)-lead(Pb) alloys have been used extensively for surface finishing in part because Pb was found to be effective in retarding Sn whisker growth in electrodeposits. Since lead-free solder alloys have been introduced, electronic manufacturers are seeking a new surface finish technology that will prevent Sn whisker growth without the use of Pb. In particular, a surface finishing technology that contains Pb should not be used with bismuth(Bi)-containing Pb-free solder alloys due to the possible formation of a low melting eutectic that could lead to thermo-mechanical degradation and fillet lifting.^[1]

There have been several studies to understand the Sn whisker growth mechanism.^[2-4] Some of the key factors that have been found to influence Sn whisker growth are: deposit thickness,^[5] deposit stress levels,^[6] substrate stress levels,^[7] additives,^[8] grain size and shape,^[9] and interdiffusion barriers.^[10] In spite of this wealth of information, basic understanding of whisker growth and its prevention does not currently exist. This research begins an attempt to understand the basic mechanism of Sn whisker growth by systematically studying correlations between deposit microstructure, whisker formation and electrodeposition parameters. We have examined the influence of Cu composition in the electrolyte and two different copper substrates on the microstructure of the Sn electrodeposit which in turn is correlated to Sn whisker growth. Grain size, grain shape, crystallographic texture and defect density were analyzed as a function of substrate, Cu content in the Sn deposit, and aging time at room temperature.

2. Experimental Procedure

2-1. Electrodeposition

Two different types of Cu substrate were prepared for Sn electroplating in order to examine their effects on deposit microstructure and Sn whisker growth. One was a free standing sample of electrodeposited copper, 250 μm thick, made from a pyrophosphate electrolyte. The second was a 40 nm thick evaporated Cu film on a Si(100) wafer. The pyrophosphate copper substrates were prepared by polishing, degreasing, magnesium oxide scrubbing, deionized water rinsing and air blast drying. The evaporated Cu substrates were not polished. Prior to tin electroplating, all substrates were immersed in 25 % sulfuric acid solution for 5 seconds to remove the oxide film and rinsed by deionized water.

Bright coatings of Sn and Sn-Cu alloys were electrodeposited from a commercial methanesulfonate electrolyte. A rotating disk electrode assembly was employed at 100 rpm to provide reproducible plating conditions and to approximate flow conditions in commercial strip plating. The 3 cm² samples were plated galvanostatically at a current density of 60 mA/cm² in one liter of solution at 25 ± 0.5 °C to a thickness of 3 μm. This correlates to a growth rate of approximately 0.05 μm / sec. The anode was a 99.999 % Sn sheet. The Cu²⁺ concentration in the electrolyte was varied from 0 to 25 x 10⁻³ mol/L by the addition of copper methanesulfonate [Cu(CH₃SO₃)₂].

Bright coatings of Sn and Sn-Cu alloys were electrodeposited from a commercial methanesulfonate electrolyte. A rotating disk electrode assembly was employed at 100 rpm to provide reproducible plating conditions and to approximate flow conditions in commercial strip plating. The 3 cm² samples were plated galvanostatically at a current density of 60 mA/cm² in one liter of solution at 25 ± 0.5 °C to a thickness of 3 μm. This correlates to a growth rate of approximately 0.05 μm / sec. The anode was a 99.999 % Sn sheet. The Cu²⁺ concentration in the electrolyte was varied from 0 to 25 x 10⁻³ mol/L by the addition of copper methanesulfonate [Cu(CH₃SO₃)₂].

2-2. Analysis

The crystallographic texture of the Sn deposits was measured by x-ray diffraction (XRD). The results are expressed in terms of a Preferred Orientation Factor, $p(hkl)$, which is defined as:

$$p(hkl) = \frac{I(hkl) / I_o(hkl)}{\frac{1}{n} \sum [I(hkl) / I_o(hkl)]}$$

where $I(hkl)$, $I_o(hkl)$, and n are the measured intensity of hkl reflections, the theoretical intensity of hkl reflections, and the number of reflections used in the analysis, respectively. In this treatment, $p(hkl)$ is the fraction of crystals that have $\{hkl\}$ plane normals perpendicular to the surface of the electrodeposit.^[11] A value of the $p(hkl)$ larger than one indicates that the hkl reflection is more highly oriented than the hkl reflection of a random powder sample.

The deposit grain size was measured by the line grid-intercept method from a 12.7 μm x 9.5 μm region near the center of the deposit using 3 x 4 grid.^[12] This provided an estimate of the

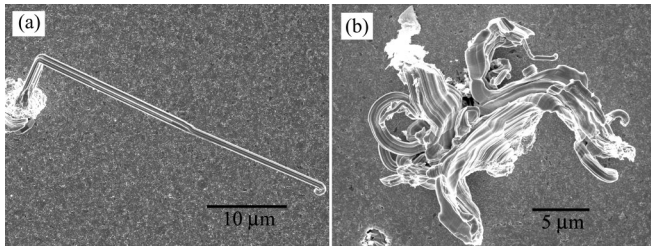


Figure 1. Types of defects on the Sn deposit: (a) a filament type Sn whisker and (b) a Sn eruption with small length whiskers.

average grain size as well as the distribution of grain sizes. To determine the Cu composition in the Sn deposits, energy dispersive x-ray spectroscopy (EDS) analysis was performed on cross sections of 10 μm thick Sn films that had been electrodeposited onto Cu evaporated Si(100). Thicker deposits were required for EDS to facilitate the analysis. The cross sections were carefully polished in separate mounts to eliminate Cu contamination. Because the deposits were multiphase, EDS data were acquired from twenty 3 μm x 16 μm areas to obtain an average over the two phases.

In this study, surface defects are defined as whiskers (Figure 1(a)) and eruptions (Figure 1(b)). The number of defects per unit area was determined as a function of Cu content in the Sn deposit and aging time at room temperature. The circular electrodeposits from the rotating disk experiments were examined using Scanning Electron Microscopy (SEM). Nine photographs were taken from each deposit along two perpendicular diameters, 4 edges, 4 mid-radii, and 1 center. Each photograph covered a region of 0.25 mm x 0.2 mm. If no defects were observed at any of these positions, the search area was expanded in all directions by ~ 0.3 mm. Whisker length was estimated from SEM micrographs at these positions.

3. Results

3-1. Preferred orientation (3 μm thick Sn deposits)

Prior to Sn deposition, the two substrates, pyrophosphate Cu and Cu evaporated Si(100), were examined by XRD for crystallographic preferred orientation. The pyrophosphate Cu had a (111) preferred orientation while the Cu evaporated Si(100) had a (100) preferred orientation. To determine the influence

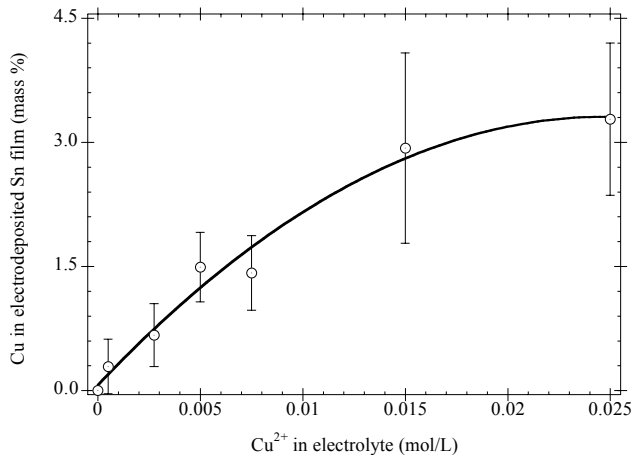


Figure 2. Cu content in the Sn deposit as a function of Cu²⁺ concentration in the electrolyte. The data point represents an average of twenty measurements from a given deposit while the error bar is the standard deviation of those measurements.

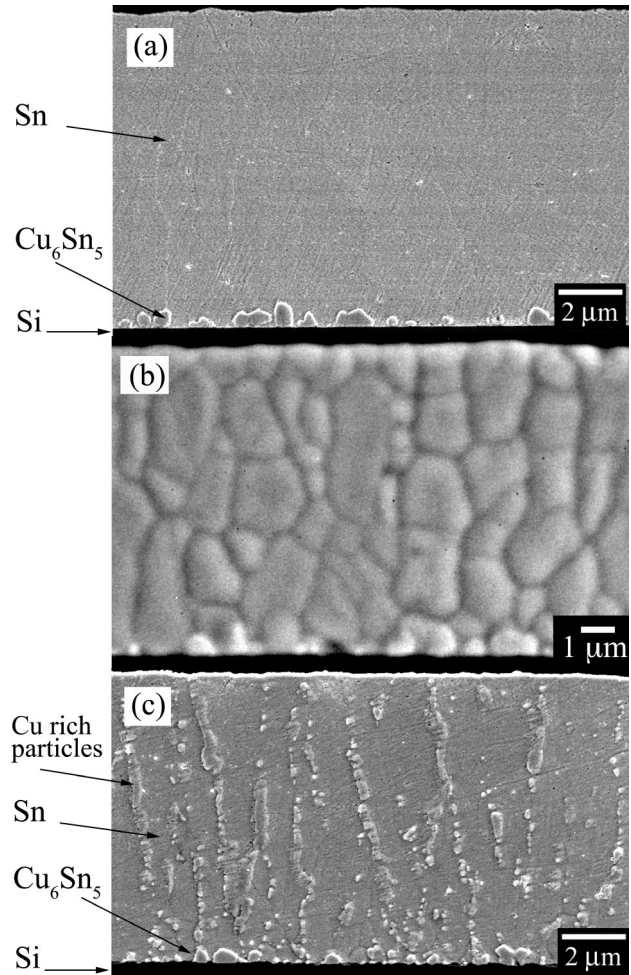


Figure 3. Cross sections of 10 μm thick Sn deposited on Cu evaporated Si(100): (a) polished pure Sn deposit, (b) pure Sn deposit following 15 s etch in 10 % HCl, and (c) polished Sn-1.5 % mass fraction Cu deposit.

of alloy composition and substrate on deposit crystallographic texture, the 3 μm thick electrodeposited Sn samples were examined using XRD. It was determined that the pyrophosphate Cu substrate led to a preferred Sn orientation of (103) while the Cu evaporated Si(100) substrate led to a (101) preferred orientation. Alloying the Sn with up to 3.3 % mass fraction of Cu did not influence the preferred orientation of the Sn deposits.

3-2. Cross section analysis for microstructures and compositions (10 μm thick Sn deposits)

The Cu content in the Sn electrodeposits and microstructure were examined as a function of Cu²⁺ concentration in the electrolyte with 10 μm thick Sn deposits on the Cu evaporated Si(100) substrate. Figure 2 shows that the Cu content in the Sn deposit increases as a function of the Cu²⁺ concentration in the electrolyte. From Figure 2, it is clear that the Cu is not depositing at the mass-transport-limited current; otherwise, Figure 2 would show a linear dependence of alloy composition on the Cu²⁺ concentration.^[13] We have observed an immersion deposit of Cu on the Sn anodes when the Cu²⁺ concentration in the electrolyte exceeds 25 x 10⁻³ mol/L, and have attributed this to an insufficient amount of Cu²⁺ complexing agent in the electrolyte. The limit on the electroactive Cu²⁺ concentration in the electrolyte limits the Cu content in the deposit. The increase in the standard deviation at the higher Cu compositions is most

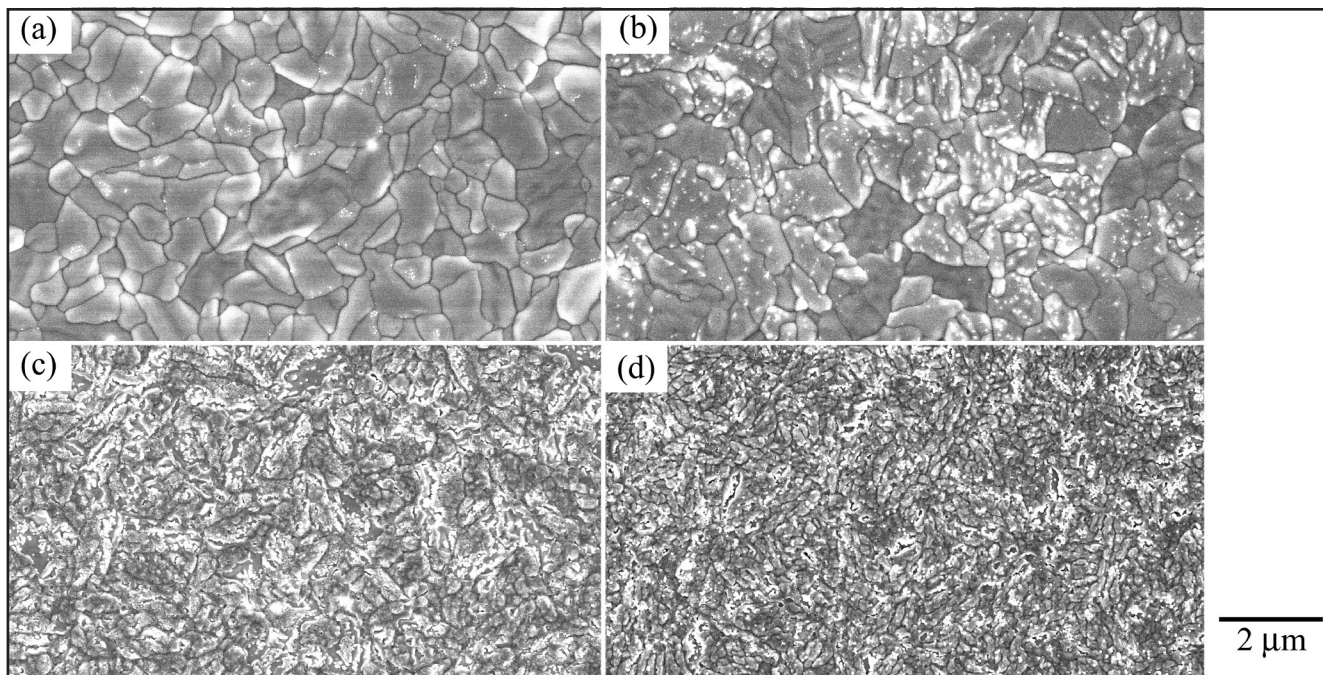


Figure 4. SEM micrographs of the as-deposited surface of 3 μm thick Sn electrodeposits containing (a) 0 %, (b) 1.5 %, (c) 2.9 %, and (d) 3.3 % mass fraction Cu. The substrate was a 250 μm thick Cu deposit from a pyrophosphate electrolyte.

likely a reflection of the inhomogeneity of the electrodeposit as it becomes two-phase as discussed below.

Figure 3 shows cross sections of two electrodeposits: (a and b) pure Sn deposit and (c) Sn-Cu alloy containing 1.5 % mass fraction Cu. In all samples, Cu_6Sn_5 is seen to form at the Sn-Cu interface as shown most clearly in Figure 3(a). The pure Sn electrodeposit is comprised of a mixture of equiaxed and elongated grains. This is clearly shown in the etched cross-section of Figure 3(b). The equiaxed grains are on the order of 1.3 μm in diameter while the elongated grains measure 4.2 μm in length and 1.6 μm in width. The grain size at the free surface appears smaller than that in the interior of the deposit (Figure 3(b)). This may indicate that grain growth processes are active below the surface.

The polished cross-section of the Sn-Cu deposit shown in Figure 3(c) shows that the grains are predominantly columnar and that Cu-rich particles decorate the grain boundaries. The Cu-rich particles are too small to analyze by EDS but are likely to be Cu_6Sn_5 . The spacing between the particles decreases as the Cu content in the Sn deposit increases. The influence of these Cu-rich particles on the deposit microstructure is under investigation.

3-3. Surface morphology and grain size (3 μm thick Sn deposits)

Determining the correlation between Sn whisker growth and Sn deposit microstructure as a function of Cu content is the primary goal of this study. Figure 4 shows the change in the as-deposited surface morphology as a function of the Cu content for 3 μm thick films electrodeposited on the pyrophosphate Cu substrate. The surface grain size depends significantly on the Cu content as shown graphically in Figure 5. The surface grain size is approximately 0.6 μm for alloys containing up to 1.5 % mass fraction Cu. This is essentially unchanged from that of the pure Sn deposit. The data shows that there is a relatively

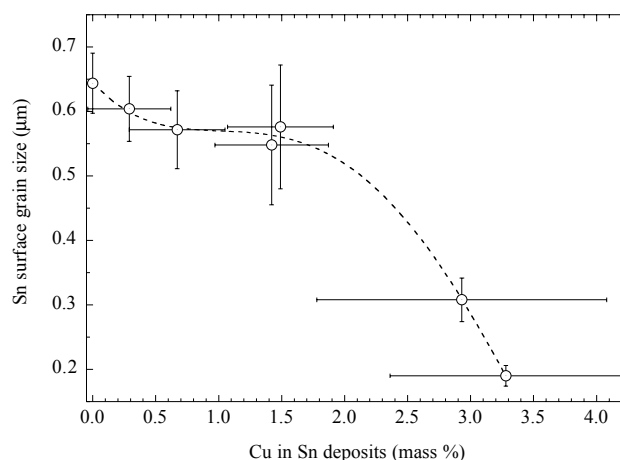


Figure 5. Grain size as a function of Cu content in the Sn-Cu deposit on the pyrophosphate Cu substrate.

large distribution of grain sizes in this composition range, as indicated by the large standard deviations. When the alloy composition exceeds 1.5 % mass fraction Cu, the surface grain size drops rather significantly and the grains appear to become more uniform (smaller standard deviation). SEM analysis of these high-Cu deposits shows that micropores and microcracks are present on the Sn deposit surface. This microstructural development with Cu addition appears to be independent of substrate type, location on the deposit, and aging time at room temperature.

3-4. Defect density (3 μm thick Sn deposits)

In this study, we have observed two types of defects on the electrodeposited Sn film: Sn whiskers (Figure 1(a)) and eruptions (Figure 1(b)). Whiskers grow out of earlier forming eruptions, but not all eruptions lead to whiskers. From the observation based on substrate types and aging times for 60 days, defects were not observed on any of the pure Sn deposits

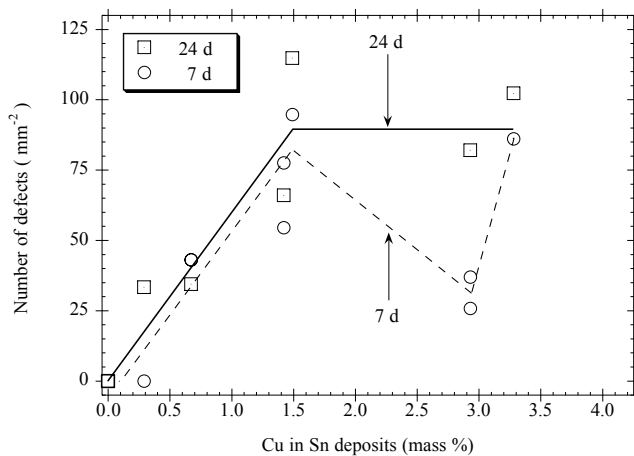


Figure 6. Number of defects (eruptions and whiskers) as a function of Cu content in the Sn-Cu deposit on the pyrophosphate Cu substrate for two aging times. Each data point is the average defect density from several locations on the electrodeposit. (See Table 1 for error ranges.)

regardless of substrate, nor were they present on Sn-Cu films deposited on the Cu evaporated Si(100) substrate. However, whiskers started to grow after 2 days from the Sn-Cu deposits on the pyrophosphate Cu substrate. All the measured values presented in Figure 2, 5, and 6 are summarized in Table 1.

Figure 6 shows the number of defects per unit area for 7-day and 24-day aged samples as a function of the Cu content in the Sn electrodeposits on the pyrophosphate Cu substrate. For a Cu content less than 1.5 % mass fraction, the number of defects increases as the Cu content increases but there does not appear to be a significant dependence on the aging time. The dip in the curve for the 7-day data is unexplained at this time even though this was observed in two independent samples.

Table 2 lists the longest Sn whiskers observed for each electrodeposit as a function of Cu content and aging time. It is clear that significant whisker growth occurs in those alloys containing a higher concentration of Cu in the deposit. The longest whisker observed was 190 μm in length. Furthermore, it was observed that the filament type of Sn whisker, as shown in Figure 1(a), is the dominant defect in the range of 2.5 % to 3.1 % mass fraction of Cu in the Sn deposit.

4. Conclusion

The influence of substrate and alloy composition on whisker growth in electrodeposited Sn and Sn-Cu films was examined. The addition of Cu^{2+} to the electrolyte resulted in the co-deposition of Cu which significantly altered the microstructure of the Sn electrodeposit. The grain size became smaller, and the microstructure changed from one containing a mixture of equiaxed and elongated grains to one that was columnar with Cu-rich particles decorating the grain boundaries. In addition, the type of Cu substrate influenced the preferred orientation of the Sn deposit. Sn films had a (103) preferred orientation when deposited on the pyrophosphate Cu substrate and a (101) preferred orientation when deposited on the Cu evaporated Si(100) substrate. Sn whiskers only grew from Sn-Cu films that had been electrodeposited onto the pyrophosphate Cu substrate. Whiskers were not observed on any of the pure Sn deposits regardless of substrate, nor were they present on Sn-Cu films deposited on

Table 1. Summary of all measurements in Figure 2, 5, and 6.

Cu^{2+} in electrolyte (mol/L)	Cu in deposit (mass %)	Sn surface grain size (μm)	Defect number (mm^{-2})	
			7 d	24 d
0	0	0.64 ± 0.05	0	0
0.00050	0.29 ± 0.33	0.60 ± 0.05	0	33 ± 25
0.00275	0.67 ± 0.38	0.57 ± 0.06	43 ± 22 $43 \pm 15^*$	34 ± 26
0.00500	1.49 ± 0.42	0.58 ± 0.10	$95 \pm 30^*$	115 ± 52
0.00750	1.42 ± 0.45	0.55 ± 0.09	55 ± 27 $78 \pm 26^*$	66 ± 41
0.01500	2.93 ± 1.15	0.31 ± 0.03	37 ± 30 $26 \pm \text{N/A}^*$	82 ± 47
0.02500	3.28 ± 0.92	0.19 ± 0.02	$86 \pm 15^*$	102 ± 58

* Only 3 regions were measured.
N/A: not available.

Table 2. Lengths of the longest Sn whisker measured as a function of alloy composition and aging time. The substrate was a 250 μm thick copper film electrodeposited from a pyrophosphate electrolyte.

Mass fraction Cu (%) in deposit	Whisker length (μm)	
	7 d	24 d
0	N/W	N/W
0.29	N/W	1
0.67	4	4
1.49	55	44
1.42	59	190
2.93	24	160
3.28	19	181

N/W: no whisker observed

the Cu evaporated Si(100) substrate after two months of observation. Thus, it appears that the presence of Cu is a necessary but not sufficient condition for whisker growth in these samples. The crystallographic texture of the Sn electrodeposit also contributes to the kinetics of whisker formation.

Reference

1. K.W. Moon, W. J. Boettinger, U.R. Kattner, C.A. Handwerker, and D.J. Lee; *Journal of Electronic Materials*, **30** (1) (2001) pp. 45-52.
2. B.Z. Lee and D. N. Lee; *Acta Materialia*, **46** (10), (1998) pp. 3701-3714.
3. K.N. Tu; *Physical Review B-Condensed Matter*, **49** (3) (1994) pp. 2030-2034.
4. U. Lindborg; *Acta Metallurgica*, **24** (2): (1976) pp. 181-186.
5. S.M. Arnold; *Plating*, **1** (53) (1966) pp. 96-99.
6. K.N. Tu; *Acta Metallurgica*, **21** (1973) pp. 347-354.
7. N. Furuta, and K. Hamamura; *Japanese Journal of Applied Physics*, **8** (12) (1969) pp. 1404-1410.
8. D.W. Endicott and K.T. Kisner; "A Proposed Mechanism for Metallic Whisker Growth." *Proceedings of the 71st AES Annual Tech. Conf.*, (Amer. Electroplaters' Society, Inc.1984) pp. J-5-1-20.
9. T. Kakeshita, K. Shimizu, R. Kawanaka, and T. Hasegawa; *Journal of Materials Science*, **17** (9) (1982) pp.2560-2566.
10. R. Schetty; "Minimization of Tin whisker Formation for Lead-Free Electronic Finishing." *Proceedings of IPC Works 2000* (IPC, 2000) pp. S-02-3-1 - 6.
11. C.S. Barrett and T.B. Massalski; *Structure of Metals Crystallographic Methods, Principles, and Data*, 3rd Ed., (New York: Pergamon, 1980) pp. 204-205.
12. H.E. Boyer and T.L. Gall; *Metals Handbook*, 9th Ed, (Metals Park: American society for Metals, 1985) pp. 35•18.
13. A.J. Bard and L.R. Faulkner; *Electrochemical Methods: Fundamentals and Applications*, (New York: John Wiley and Sons, Ltd., 1980) pp. 288.